CEBAF PROPOSAL COVER SHEET

This Proposal must be mailed to:

CEBAF
Scientific Director's Office
12000 Jefferson Avenue
Newport News, VA 23606

and received on or before OCTOBER 30, 1989

A. TITLE: Study of Coincidence Reactions in the Dip and Delta-Resonance Regions

B. CONTACT PERSON: Hossain Baghaei

ADDRESS, PHONE AND BITNET:

Nuclear Physics Group, Univ. of Massachusetts, Amherst, MA 01003 HBAG@UMASS, (413)545-2480

C. THIS PROPOSAL IS BASED ON A PREVIOUSLY SUBMITTED LETTER OF INTENT

[X] YES
[ ] NO

IF YES, TITLE OF PREVIOUSLY SUBMITTED LETTER OF INTENT

Same

D. ATTACH A SEPARATE PAGE LISTING ALL COLLABORATION MEMBERS AND THEIR INSTITUTIONS

==========

(CEBAF USE ONLY)

Letter Received 10-31-89

Log Number Assigned PR-89-015

By KES

contact: Baghaei

H. Baghaei, R.S. Hicks, A. Hotta, R.A. Miskimen, G.A. Peterson, and T. Tamae
Department of Physics and Astronomy
University of Massachusetts at Amherst
Amherst, Massachusetts 01003

October 28, 1989

Dear members of the PAC,
At present the role of multinucleon absorption processes in deep inelastic electron scattering and the properties of the Δ resonance in nuclei are poorly understood and potentially very interesting and exciting subjects. The interest in this field is shown by the three CLAS experiments proposed to study various aspects of the (e,e') reaction mechanism.

- 'Coincidence Reaction Studies with the LAS' (spokesman: L. Weinstein, MIT) proposes to examine the various (e,e') reaction mechanisms in the quasielastic, dip, quasifree delta, and quasifree resonance regions at four beam energies from 600 to 2000 MeV with five targets from Deuterium to Lead.

- 'Study of Coincidence Reactions in the Dip and Delta-Resonance Regions' (spokesman: H. Baghaei, UMass) proposes to study the different processes that contribute to electron scattering in the dip and quasifree delta resonance regions and also to investigate the possible medium modifications of the Δ in nuclei at various energies with four targets from Helium to Lead.

- 'Electroexcitation of the $\Delta(1232)$ in the Nuclear Environment' (spokesman: R. Sealock, UVa) proposes to examine the position, width, and form factor of the delta resonance as a function of A, and Q^2.

These experiments overlap significantly. They each intend to examine all reaction channels for a given (overlapping) set of electron kinematics. They will use similar targets, beam energies, luminosities, CLAS polarity, and triggering schemes. We expect that most of the data will be taken simultaneously, initially triggering data acquisition by detection of an electron so as to have an unbiased look at the hadronic final state. Later, we will use more selective triggers, that include hadronic requirements, to emphasize one or more aspects of these experiments. We plan to collaborate during the next few years on more thorough modeling of the CLAS acceptances and efficiencies as they affect these experiments so that we can optimize the various experimental plans.

Yours Sincerely,

Hossain Baghaei

Hossain Baghaei
Richard Sealock
Larry Weinstein

Study of Coincidence Reactions in the Dip and Delta-Resonance Regions

H. Baghaei*, R. S. Hicks, A. Hotta, R. A. Miskimen,
G. A. Peterson, and T. Tamae

Department of Physics and Astronomy
University of Massachusetts at Amherst
Amherst, Massachusetts 01003

Abstract

We propose to use CEBAF Large Acceptance Spectrometer (CLAS) to do a systematic study of ω and q dependence of the cross sections for coincidence reactions with many hadrons in the final state, e.g. (e,e'N), (e,e'NN), (e,e'Nπ) etc., in the dip and delta resonance regions for several nuclear targets (e.g. ^{3}He, ^{12}C, ^{40}Ca and ^{208}Pb). Results of the intermediate energy single arm (e,e') and coincidence (e,e'p) experiments in these regions indicate the importance of the multinucleon absorption processes and the role of $\Delta(1232)$-resonance in the reaction. The goals of our program are: **(1)** to isolate the different multi-nucleon absorption processes and investigate their ω and q dependence; and **(2)** to study the $\Delta(1232)$ production and its interaction with nucleons. We will measure the momentum dependence of the (e,e'Nπ) reaction to investigate the possible modification of the delta and its dominant magnetic form factor in the nuclear medium. Even though here we propose to use an electron beam, we hope to extend this program to study reactions with tagged photons. In this proposal we are giving some preliminary estimates of the count rates for three different beam energies.

* Contact person

I. Motivation

Inclusive deep inelastic electron scattering from nuclei at intermediate energies generally shows two broad peaks corresponding to quasifree elastic scattering from the nucleon (QE) and quasifree $\Delta(1232)$ resonance production, with a "dip" region between them. The inclusive cross section at the QE peak and at the Δ resonance is predominantly due to one-body processes. However, the results of recent inclusive (e,e') and exclusive (e,e'p) electron scattering experiments at the dip and delta resonance regions indicate that many-body effects play an important role in these reactions.

Multinucleon Absorption Processes: In the dip region the measured inclusive cross section shows an excess compared to one-body calculations augmented by meson exchange currents.[1-3] The ^{12}C(e,e') cross section as a function of the energy transfer to the nucleus ω for a beam energy of E_i = 680 MeV and scattering angle θ_e= 36°is shown in Fig. 1, and is compared to a theoretical calculation by Laget. The solid curve represents the sum of the quasielastic (dash-dot) meson-exchange current (dot) and pion production (dash) curves. According to this calculation, in the dip region at $\omega \simeq$ 250 MeV, the one-body process contribution is about 20% of the total strength. These results certainly indicate the importance of the many-body processes.

To isolate the different processes that contribute to (e,e') reaction requires the measurement of coincidence cross sections. In Fig. 2 the coincidence cross section as a function of the missing energy is shown for the reaction ^{12}C(e,e'p) at the dip region[4], for the experiment done at M.I.T.-Bates at kinematics E_i= 460 MeV, ω = 200 MeV and $\vec{q}$ = 400 MeV/c. It indicates a pronounced p-shell peak at missing energy about 18 MeV, a s-shell peak at missing energy between 30 to 70 MeV and a strong and nearly uniform strength to the highest measured missing energy. Takaki[5] has recently investigated the contributions of the many body processes to the (e,e'p) reaction at this kinematics. His results, Fig. 3, show that the cross section for the two-body process (solid curve) at missing energies above 100 MeV is negligible. He suggests that to understand the data one has to include processes

which involved three or more nucleons. His qualitative investigation of the three-nucleon process (dashed and dash-dotted curves) indicates that it populates the region of $\epsilon_m \geq 100$ MeV.

The contribution of multinucleon processes is also seen in ^{3}He(e,e'p) data in the dip region measured at Saclay.[6] The missing energy spectra, Fig. 4, clearly show a broad peak beyond the 1s-shell knockout due to three-body break up. Curves are the results of a two-body calculation by Laget.

It is clear from these (e,e') and (e,e'p) results that in the dip region processes other than quasielastic single-nucleon knockout process are present and indeed dominate. To study these processes in more details we have to do coincidence reactions with many particles in the final state, which are very time consuming with existing low duty factor accelerators and limited-acceptance spectrometers.

Evidence for multinucleon absorption is also seen in delta resonance. The A dependence of the delta peak in the (e,e') reaction for several light nuclei has been studied at M.I.T.-Bates by O'Connell *et al.*[7]. The measured cross sections per nucleon, shown in Fig. 5, reveal several features: **(1)** The cross sections scale with A; **(2)** The location of the peak is lower than for hydrogen; **(3)** the peak width ($\simeq$ 250 MeV) is larger than that obtained by simply folding the width of the free Δ peak ($\simeq$ 120 MeV) with the observed width of the quasifree peak ($\simeq$ 100 MeV); and **(4)** the integrated cross section per nucleon of the Δ peak is enhanced by 34% relative to the free nucleon. These results indicate that processes other than one-body process contribute to the (e,e') reaction, and that the properties of the delta in the nuclear medium are modified by the effects of the Fermi motion, Pauli blocking and the N-Δ interaction. Theoretical calculations generally underestimate the data. For example, Fig. 6 and Fig. 7 show calculations by Koch *et al.*[8] and Chen and Lee[9] for ^{12}C(e,e'). These calculations which include medium effects in the Δ-excitation, in the framework of Δ-hole model, reproduce the broad shape of the peak relatively well, but both predict cross sections that are small. These results suggest the presence of more complex multinucleon processes, and perhaps a better treatment of the modification of the Δ in the nuclear medium.

A preliminary attempt[10] to disentangle the different reaction processes, has been made at M.I.T.-Bates by measuring the ^{12}C(e,e'p) coincidence reaction in the delta resonance region. The missing energy spectrum obtained for two different kinematics (I and II) is shown in Fig. 8. For kinematics I the beam energy was 460 MeV, ω = 275 MeV, $|\vec{q}|$ = 401 MeV/c, and the electron scattering angle θ_e was 60°, corresponding to a point roughly halfway between the dip region and the Δ resonance peak. Protons were detected at −23.6°. For kinematics II, the electron kinematics were fixed at the maximum of the quasifree Δ production peak: E_0 = 647 MeV, ω = 382 MeV, $|\vec{q}|$ = 473 MeV/c and θ_e = 39.5°. Protons were detected at −20.8°. These results clearly show strength in three different regions: **(1)** The region below 30 MeV missing energy ϵ_m which is dominated by the quasifree knockout process; **(2)** The region above the real pion production threshold ($\epsilon_m \geq$ 165 MeV), which is dominated by Δ(1232) resonance production and distinguished by a sharp increase in the coincidence cross section at pion threshold; and **(3)** The region between 30 MeV and 165 MeV. From the trends observed in (γ, p) data (see below) and the absence of real pions we conclude that region (3) is populated by two- or many-nucleon knockout processes. To estimate the contribution of the region (3) to the total process the missing energy spectra are fitted with two Gaussians. The solid curves in Fig. 8 show the sum of the fits. The integrated strength under the Gaussian fit to region (3) accounts for 30% (12%) of the yield for kinematics I (II). Such multinucleon processes, which can't take place in hydrogen, may be able to account for the enhancement observed in the cross section per nucleon over that of the hydrogen (Fig. 5).

The ^{12}C(e,e'p) results shown in Fig. 8 demonstrate the ability of the coincidence (e,e'p) measurements to isolate, to some extent, the contribution of the different processes to the reaction mechanism. But from this data we cannot separate two- and many-body processes from each other and furthermore cannot eliminate the possibility that the many-nucleon knockout strength may extend to the pion production region. Indeed, Takaki's calculations[5] suggest that the ratio of three-body to two-body cross sections at their respective peaks in the missing energy spectrum for kinematics I is about 1.1. This ratio for kinematics II is about 1.8.

The ^{12}C(e,e'p) spectra are qualitatively similar to the (γ,p) spectra measured in the delta region by Homma *et al.*[11], shown in Fig. 9. Homma *et al.* measured proton momentum spectra for several light nuclei at different tagged photon energies and fit each spectrum with Gaussians. From the variation of the peak centroids with incident photon energy and from comparison with the deuterium data they concluded that the peak at lower proton momentum (corresponding to the higher missing energy peak in the ^{12}C(e,e'p) data) is due to the reaction γ +"N"$\rightarrow$ p + π, and that the smaller peak at higher proton momentum is due to the reaction γ + "pN"$\rightarrow$ p + N. Here "N" and "pN" denote the quasifree nucleon and quasifree two nucleon systems in the nucleus. Subsequent measurements of the (γ,pn), (γ,pp) and (γ,pπ) reactions by Kanazawa *et al.*[12] show several features: (1) The contribution of many-nucleon knockout processes beyond pion threshold (Fig. 10); (2) the back-to-back nature of the emitted protons and neutrons (Fig. 11); and (3) the dominance of the (γ,pn) over (γ,pp) reaction (Fig. 12).

Recent measurements of the ^{4}He(γ,pn)X reaction indicate that this reaction cannot be solely attributed to absorption on a quasi-deuteron pair. Maruyama[13] has argued that absorption on 2N, 3N or even 4N could contribute to the 'small peak' seen in (γ,p) data and can explain the back-to-back emission of neutrons and protons. In Fig. 13 the distribution of the correlation angle between the outgoing protons and neutrons is compared with the results of calculations of absorption on 2N, 3N and 4N constituents. The results show that the discrimination of 2N absorption from 3N and 4N absorption is difficult only by kinematical analyses using momenta of two outgoing particles.

In summary, Existing electron scattering and tagged photon data indicate the importance of multinucleon absorption of virtual and real photons. To study these processes, and to answer to the question of how many nucleons are involved in the absorption of a photon, we have to isolate different processes by measuring coincidence reactions with multi-particle in the final state and also study their ω and q dependence. With 100% duty factor, a tagged photon facility, and the Large Acceptance Spectrometer CEBAF will be ideal for these kind of experiments. Our preliminary interest is to study electron-scattering reactions, e.g. (e,e'N), (e,e'NN),

(e,e'Nπ) etc., but we hope to later extend this program to study these reactions with a tagged photon beam.

Momentum dependence of the pion production reaction : The $\Delta(1232)$-resonance, the first and best resolved nucleon resonance, plays an important role in medium energy nuclear reactions. Its production, propagation and modification in the nuclear medium constitues an important subject in nuclear physics. As mentioned before, the existing data suggest a modification of the delta properties in the nucleus, which can be due to the effects of Fermi motion, Pauli blocking, and Δ-N interactions. We plan to investigate this possibility by measuring the momentum dependence of the (e,e'Nπ) cross section and seeking deviations from what is expected for free nucleons. Since the non-resonance contribution is much smaller for neutral pion production, it would be desirable for CLAS to have comprehensive detection capability for neutral pions.

The elementary p(e,e'p)π process in the delta region can be represented by diagrams shown in Fig. 14. Diagrams (a)-(c) are the non-resonance terms (Born terms) and diagram (d) is the resonance term which is assumed to proceed through the delta production channel. Measurements of the Q^2-dependence of the γNΔ vertex form factors are essential for testing microscopic models of the nucleons. The γNΔ vertex can be characterized by three electromagnetic multipoles: magnetic dipole M1, electric quadrupole E2, and Coulomb quadrupole C2. The $\Delta(1232)$ is dominantly magnetic and M1 is usually expressed in terms of G_M^* which is analogous to the nucleon elastic magnetic form factor G_M:[14]

$$G_M^{*2} = C\frac{p_\pi^c}{q^c}\Gamma(M1)^2$$

where C is a constant, $p_\pi^c(q^c)$ is the pion (virtual photon) momentum in the C.M. of the outgoing hadrons, and Γ is the width of the delta. The ratio of the $G_M^*/3G_D$, shown in FIg. 15, indicates that G_M^* is dropping off faster with Q^2 than the dipole expression for the nucleon form factor $G_D = 1/(1+Q^2/0.71)^2$. The curves represent the results of quark model calculation by Foster and Hughes (dashed line)[15] and Schroeder *et al.* (solid line).[16] The other two form factors, E2 and C2, are poorly determined, and are expected to be 5-10% of the M1. Although such

contributions may be small they indicate significant violations of SU(6) symmetry, and of the spherical quark model.[14-17] Attempts to measure E2 and C2 form factors with a good accuracy are underway at M.I.T.-Bates.

The next step will be to study these multipoles in nuclei. This can be done by measuring the momentum transfer dependence of the pion production cross section. Since pion production cross section measured by (e,e') experiments include two-or many-body processes and tail of the quasielastic peak, such measurements are unsuitable for studying the delta properties in nuclei. On the other hand, CLAS will permit isolation of (e,e'Nπ) process, and afford the opportunity to study modification of the delta. Of course, it will be required to separate the non-resonance contributions and to correct for final state interactions.

Δ-N interaction: The (γ, p) cross sections measured by Homma *et al.*[11], shown in Fig. 9, have been integrated over proton momentum yielding. The results are shown in Figs. 16a and 16b. Fig. 16a is for single nucleon absorption, and Fig. 16b for absorption on assumed two-nucleon pair. Homma *et al.* concluded that the contribution of the delta resonance is dominant, and that two-body processes proceed through the Δ-nucleus interaction. We propose to study the (virtual) photon energy dependences of (e,e'N), (e,e'NN), (e,e'Nπ) etc. cross sections and investigate the role of delta production in these processes. For example, since two-body knockout can proceed via the following process:

$$e + N \rightarrow e' + \Delta$$
$$\Delta + N \rightarrow N + N \ ,$$

the data could be used to study the Δ-nucleon interaction in A>1 nuclei.

II. Count Rates Estimates

Here we give an estimation of the count rates for (e,e'pn), (e,e'pp), and (e,e'pπ) reactions for three different beam energies: 647 MeV, 1200 MeV and 2000 MeV. All estimations are done for ^{12}C nucleus and assuming a luminosity of 10^{34} cm^{-2}sec^{-1} for the CLAS detector.

Since we are interested in studying the ω and q dependence of the different reaction processes, the count rates have been calculated for fixed ω and q. Therefore, the energy and angle of the scattered electron is assumed to be within a restricted range of the total CLAS acceptance. Of course one of the most basic advantages of CLAS is the ability to map out simultaneously an extensive range of ω and q during a single measurement with one beam energy. Such a measurement could cover the entire region from the QE peak to $\Delta(1232)$ peak.

The selected kinematics are given in Table I. To facilitate the estimation of the count rates, and also to tie in these measurements with the existing data from other laboratories, the kinematics I is chosen to be the same as that of the ^{12}C(e,e'p) experiment at Bates.

Table I. Experimental Kinematics

Kinematics	E_o (MeV)	Θ_e (deg)	ω (MeV)	$\vec{q}$ (MeV/c)	Q^2 (GeV/c)^2
I	647	39.5	382	473	0.08
II	1200	40	538	813	0.37
III	2000	30	709	1093	0.69

Note that for each beam energy and electron scattering angle the chosen ω and q are correspond to the maximum of the $\Delta(1232)$-resonance peak for a free nucleon. In these kinematics the (e,e'pπ) rates are maximum and (e,e'NN) rates are at their lowest values. In the future we will provide count rates for a broader range of kinematics: from the dip region, where (e,e'NN) processes are dominant, to the delta peak.

For a given polar angle θ_e, the azimuth angle ϕ_e can have any value within the ϕ acceptance of the CLAS. We assumed:

$$\Delta\theta_e = \pm 50\ mrad$$

$$\Delta\phi_e = 0.70 \times 2\pi\ rad$$

$$\Delta\Omega_e = 440\ msr$$

$$\Delta p_e/p_e = \pm 5\%$$

In the following section we describe how we approximated the cross sections.

Coincidence Cross Sections

For kinematics I, the ^{12}C(e,e'pπ) cross section was assumed to be

$$d^5\sigma(e,e'p\pi) \sim \frac{1}{4\pi} d^4\sigma(e,e'p),$$

where d$^4\sigma$(e,e'p) is the cross section for missing energies above pion threshold, $\epsilon_m \geq 165$ MeV, in Fig. 8. Similarly the ^{12}C(e,e'pn) cross section is approximately

$$d^5\sigma(e,e'pn) \sim \frac{1}{4\pi} d^4\sigma(e,e'p),$$

where d$^4\sigma$(e,e'p) in this case is the cross section for missing energies below pion threshold. For other two beam energies the (e,e'p) cross sections were estimated as follows.

(1) (e,e'pπ) cross section: For ^{12}C(e,e'pπ) process the cross section is approximated by:

$$d^5\sigma(e,e'p\pi) \sim \frac{1}{4\pi} d^4\sigma(e,e'p)$$

where $d^4\sigma/dE_e d\Omega_e dE_p d\Omega_p$ is the cross section for (e,e'p) reaction in the pion production region, which has been expressed as[10]

$$\frac{d^4\sigma}{dE_e d\Omega_e dE_p d\Omega_p} = \int K \overline{\sum_{fi}} |M_{e\Delta}|^2 S(\vec{p}_i, \epsilon_m) d^3p_i \ .$$

In this equation the integral is over the nucleon initial momentum p_i, and K is a kinematical factor. The spectral function $S(\vec{p}_i, \epsilon_m)$ was modelled with harmonic oscillator momentum distributions and δ-functions in missing energy located at the centroids of the experimental shell energies of the p-shell and s-shell. For $M_{e\Delta}$ we utilized the amplitude of the elementary reaction, $e + p \rightarrow e + \Delta \rightarrow e + p + \pi$. Fig. 17 shows results of such calculation for (e,e'p) data measured at Bates-M.I.T. In Figs. 18 and 19 the (e,e'p) cross sections for kinematics II and III are shown respectively.

(2) (e,e'NN) cross section: For ^{12}C(e,e'pn) process the cross section is approximated by:

$$d^4\sigma(e,e'pn) \sim \frac{1}{4\pi} d^3\sigma(e,e'p),$$

where $d^3\sigma(e,e'p)/dE_e d\Omega_e \Omega_p$ is the (e,e'p) cross section for two-nucleon absorption reaction, calculated by using virtual photon theory and under the assumption that the excitation of the delta is dominantly transverse:

$$\frac{d^3\sigma(e,e'p)}{dE_e d\Omega_e d\Omega_p} = \Gamma_v \frac{d\sigma(\gamma,p)}{d\Omega_p},$$

where

$$\Gamma_v = \frac{\alpha}{2\pi^2}(\omega - \frac{Q^2}{2m})(\frac{E_i - \omega}{E_i})\frac{1}{1-\epsilon}\frac{1}{Q^2}$$

can be interpreted as the flux of virtual photons per scattered electrons in dΩ_e and dE_e. In these expressions $Q^2 = q^2 - \omega^2$, E_i is the beam energy, and $\epsilon = (1 + 2\frac{\vec{q}^2}{Q^2} tan^2(\theta_e/2))^{-1}$ is the photon polarization parameter. The differential cross section $d\sigma/d\Omega_p$ is for real photon absorption by ^{12}C, estimated according to quasi-deuteron model:

$$\frac{d\sigma}{d\Omega_p} = (\frac{NZ}{A}L)(\frac{d\sigma}{d\Omega_p})_d,$$

where L is the Levinger factor and $(d\sigma/d\Omega_p)_d$ is the cross section for photodisintegration of deuteron.

To estimate the ^{12}C(e,e'pp) cross section we multiplied the (e,e'pn) cross section by a factor of 0.10, based on the real tagged photon data shown in Fig. 12. Assuming a 5%-10% efficiency for the neutron detector, the count rate for (e,e'pp) reaction will be comparable to the (e,e'pn) process. The count rates are summarized in Table II.

Table II. Count rate

Kinematics	process	E_f (MeV)	Θ_q (deg)	p_p (MeV/c)	p_π (MeV/c)	counts (hr^{-1})
I	(e,e'pn)	265	20.8	820	348	10
I	(e,e'pπ)	265	20.8	438	248	238
II	(e,e'pn)	662	31.5	1190	378	5
II	(e,e'pπ)	662	31.5	365	448	890
III	(e,e'pn)	1291	36.2	1307	215	2
III	(e,e'pπ)	1291	36.2	552	541	4944

Accidental Rate

To estimate the accidental coincidence rate we need to know the inclusive cross sections and double coincidence cross sections. The accidental rate for the (e,e'pp) reaction is estimated by:

$$R_{acc} \simeq R_e R_{p1} R_{p2} (\Delta\tau/DF)^2 + R_{ep1} R_{p2} (\Delta\tau/DF) + R_{ep2} R_{p1} (\Delta\tau/DF)$$

where R_e and R_p are the singles rates for (e,e') and (e,p) reactions. The rate R_{ep} is for true double coincidence (e,e'p). The time resolution, $\Delta\tau$ was assumed to be 10 ns, and the duty factor DF=1. For the proton single rates we used the program developed by O'Connell. The estimated ^{12}C(e,e') cross section for $E_0 = 647$ MeV was based on the previous ^{12}C(e,e'p) data at the delta region. For higher beam energies the (e,e') cross section was estimated by rescaling CEA data.[15] In all cases we found that the accidental rates are negligible compare to the true coincidence rates.

III. Experimental Plan

As noted above we plan to use the Large Acceptance Spectrometer for these measurements. With its large solid angle and momentum acceptances the CLAS detector should be ideal for these kind of experiments. Its relatively low luminosity, which will help to achieve a good signal to noise ratio, will be compensated by its large acceptances. Its momentum resolution ($\leq 1\%$) will not be a problem for experiment proposed here. The CLAS standard detection apparatus will be used for detecting and identifying charged particles. For detection of the neutrons we plan to use a set of thick plastic scintillators which will be located close to the hall walls.

We plan to use several targets ranging from few-body systems up to heavy nuclei. These targets can be Helium, Carbon, Calcium, and Lead. Of course, measurement would also be performed on ^{1}H and ^{2}H for normalization and calibration purposes.

The trigger for this experiment should be as general as possible, consists of a combination of indicators for the detection of an scattered electron (unbiased trigger). However, since the data acquisition system would be able to handle much lower rate than the detector system can, we may have to choose a more restricted hardware trigger. The exact nature of this trigger remains to be established.

The count rates presented here, for three specific sets of kinematics at the delta peak for ^{12}C target, indicate that to get 1000 counts for the ^{12}C(e,e'pp) reaction will require 100 (500) hours for kinematics I (kinematics III). Since the rate for (e,e'pπ) reaction is much higher than (e,e'pp) reaction, we will probably have to sample a prescaled fraction of pion events. In the future, by modeling the CLAS acceptances we would carry out a more complete estimate, for different targets and a broader range of kinematics.

References

[1] P. Barreau *et al.*, Nucl. Phys. **A402**, 515 (1983).

[2] J. W. Van Orden and T. W. Donnelly, Ann. Phys. (N.Y.) **131**, 451 (1981); T. W. Donnelly *et al.*, Phys. Lett. **76B**, 393 (1978).

[3] J. M. Laget, From Collective States to Quarks in Nuclei, Lecture Notes in Physics, vol. 137, ed. by H. Arenhövel and A. M. Saruis, Springer, Berlin (1981).

[4] R. W. Lourie *et al.*, Phys. Rev. Lett. **56**, 2364 (1986).

[5] T. Takaki, Physical Review **C39, 359 (1989).**

[6] C. Marchand *et al.*, Phys. Rev. Lett. **60**, 1703 (1988).

[7] J. S. O'Connell *et al.*, Phys. Rev. Lett. **53**, 1627 (1984); Phys. Rev. **C35**, 1063 (1987).

[8] J. H. Koch and N. Ohtsuka, Nucl. Phys. **a435**,765 (1985).

[9] C. R. Chen and T. S. Lee, Physical Review **C38, 2187 (1988).**

[10] H. Baghaei, Ph.D. thesis, M.I.T. (1987); Physical Review **C39, 177 (1989).**

[11] S. Homma *et al.*, Nucl. Phys. **A446**, 241c (1985); Phys. Rev. Lett. **53**, 2536 (1984); Phys. Rev. **C27**, 31 (1983).

[12] M. Kanazawa *et al.*, Phys. Rev. **C35**, 1828 (1987).

[13] K. Maruyama, Invited talk at the 4-th workshop on "Perspective in Nuclear Physics at Intermediate Energies", at Triete, Italy, MAy 8-12 (1989).

[14] V. Burket, CEBAF-PR-87-025 (1987).

[15] F. Foster, G. Hughes, Rep. Prog. Phys. **46**, 1445 (1983).

[16] H. Schroeder, 1986 CEBAF Summer Workshop (1986).

[17] F. Foster, G. Hughes, Z. Phys. **C14**, 123 (1982).

[18] J. W. Lightbody Jr., Rep. of the 1985 CEBAF summer study, pp. 10-24 (1986).

[19] K. C. Stanfield *et al.*, Phys. Rev. **C3**, 1448 (1971).

Figure Caption

Figure 1. The ^{12}C(e,e′) cross section compared to a theoretical calculation by Laget. The solid curve represents the sum of the quasielastic (dash-dot) meson exchange current (dot) and pion production (dash) curves.

Figure 2. The missing energy spectrum for ^{12}C(e,e′p) reaction in the dip region (Ref. 4).

Figure 3. Missing energy spectra in the dip region calculated by Takaki. Solid curve: two-nucleon absorption in the zero range assumption. Dashed curve: three-nucleon absorption in the zero range assumtion. Dash-dotted curve: three-nucleon absorption through real pion production. The peaks of all curves are normalized to 10 (in arbitrary units).

Figure 4. The missing energy spectrum for ^{3}He(e,e′p) reaction. The dotted (solid) histograms show data before (after) radiative corrections. Curves are theoretical predictions by Laget. Simple PWIA, dashed curve; DWIA, dot-dashed curve; DWIA + MEC, solid curve. The arrow indicates the position expected for D(e,e′p) reaction (Ref. 6).

Figure 5. The (e,e′) cross section per nucleon for hydrogen and several light nuclei (Ref. 7).

Figure 6. The Δ-hole calculation of ^{12}C(e,e′) cross section from Ref. 8. Solid curve: full calculation; long dashes: calculation with no spreading potential; dotted: sum of non-resonant contributions; short dashes: sum of single-nucleon cross section; dash-dot: quasifree nucleon knockout cross section.

Figure 7. The calculated ^{12}C(e,e′) cross sections (solid curves) are from Ref. 9. The dashed curves are from the quasifree nucleonic process, and dotted curves are from the quasifree Δ production, and dash-dotted curves are from the $\gamma NN \rightarrow NN$ two-body process.

Figure 8. The missing energy spectrum for the ^{12}C(e,e'p) reaction in the delta region for two choices of kinematics. The solid curve is the sum of two Gaussians fit to the two peaks (Ref. 10).

Figure 9. The momentum spectrum of the proton for $^{12}C(\gamma,p)$ reaction at photon energy of 357 MeV and θ_p = 30 °(Ref. 11). The solid curve is the sum of two Gaussians fit to the two peaks.

Figure 10. Tagged photon coincidence studies on ^{9}Be (right) and the deuteron (left). From top to bottom, the reaction are (γ,p), $(\gamma,p\gamma)$, (γ,pn), $(\gamma,p\pi)$ and (γ,pp) (Ref. 12).

Figure 11. The angular of correlation between the protons and neutrons in the reaction ^{9}Be(γ,pn) at the photon energy of 247 MeV and θ_p = 30 °. The solid curve is the results of a Monte Carlo calculation.

Figure 12. The ratio of the cross section of the reaction γ + "pp" → p + p to the reaction γ + "pn" → p + n as a function of the photon energy for ^{9}Be and ^{12}C.

Figure 13. The distribution of correlation angle between the protons and neutron. Calculations for 2N, 3N, and 4N are shown (Ref. 13).

Figure 14. Feynman diagrams that dominate low-energy electroproduction in the one-photon exchange approximation: (a-c) Born terms, (d) isobar term.

Figure 15. Ratio of the magnetic form factor for $\gamma N\Delta$ vertex to the nucleon form factor.

Figure 16. The cross section, integrated over proton momentum, for: (a) the quasifree reaction γ + "N" → p + π at θ_P = 30°for ^{1}H, ^{2}H, ^{4}H, ^{9}Be, ^{12}C, and ^{16}O as a function of the photon energy; (b) the quasifree reaction γ + "pN" → p + N at θ_P = 30°for ^{2}H, ^{4}H, ^{9}Be, ^{12}C, and ^{16}O as a function of the photon energy.

Figure 17. The calculated cross section for ^{12}C(e,e'p) reaction compared to data in the delta region. The dashed curve is the result of the quasifree calculation

with harmonic oscillator momentum distributions, the dotted curve is a three-body phase space result and the solid curve is their sum (Ref. 10).

Figure 18. The calculated cross section for ^{12}C(e,e'p) reaction in the delta peak for Kinematics II.

Figure 19. The calculated cross section for ^{12}C(e,e'p) reaction in the delta peak for Kinematics III.

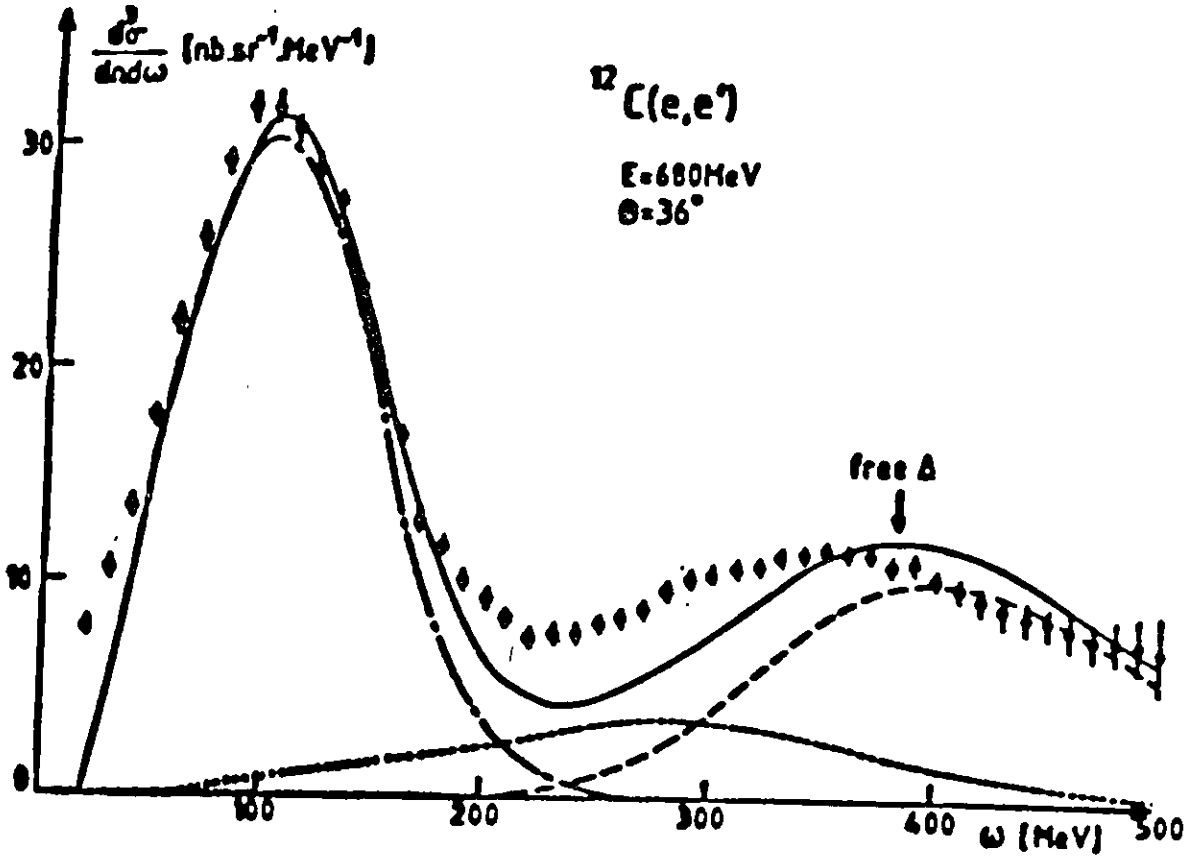
$\frac{d^2\sigma}{d\Omega d\omega}$ [nb.sr^{-1}.MeV^{-1}]
^{12}C(e,e')
E=680MeV
θ=36°
free Δ
30
20
10
0
100
200
300
400
ω [MeV]
500

Figure 1.

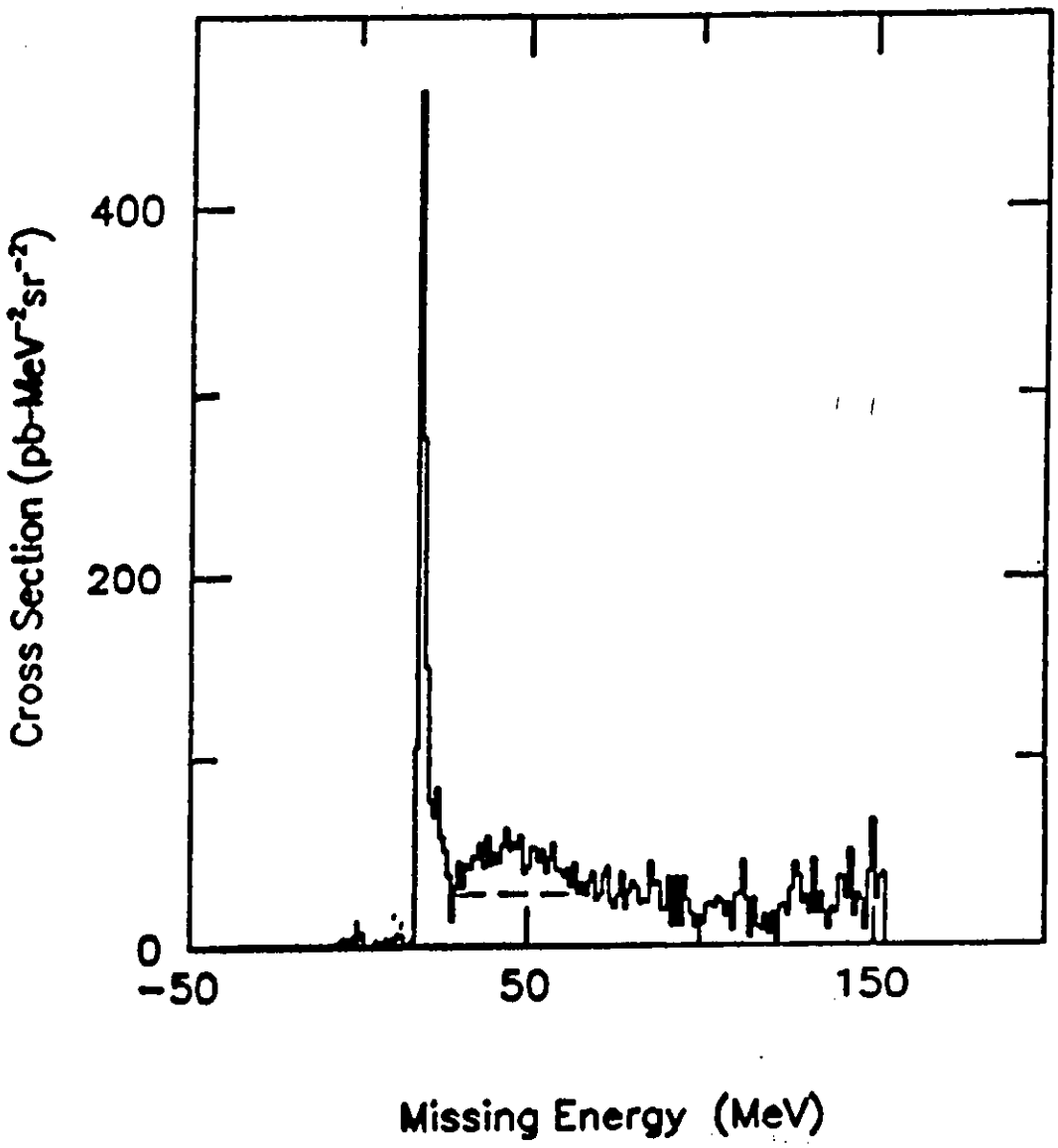
Cross Section (pb-MeV⁻²sr⁻²)
400
200
0
-50
50
150
Missing Energy (MeV)

Figure 2.

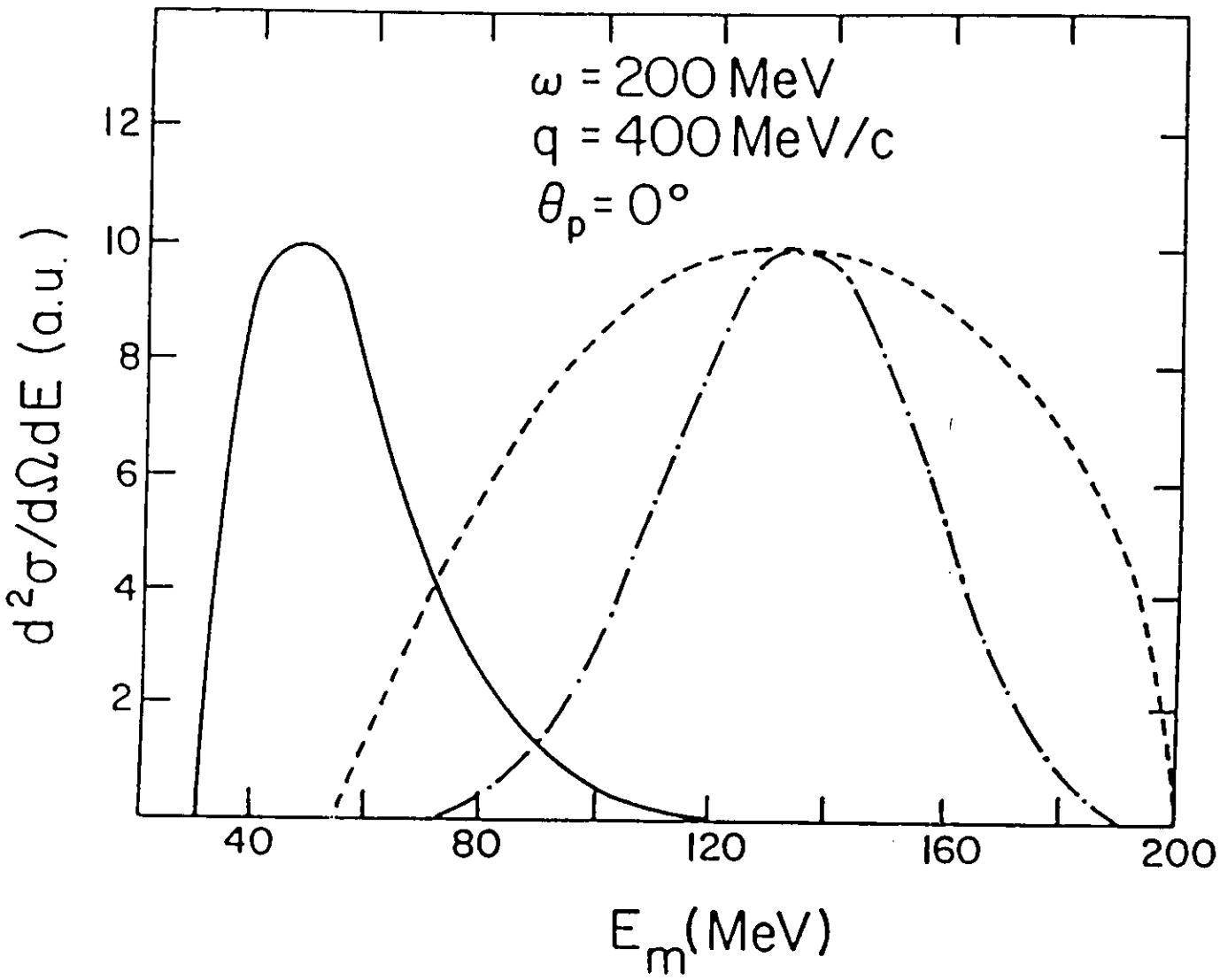
ω = 200 MeV
q = 400 MeV/c
θp = 0°
d²σ/dΩdE (a.u.)
12
10
8
6
4
2
40
80
120
160
200
Em(MeV)

Figure 3.

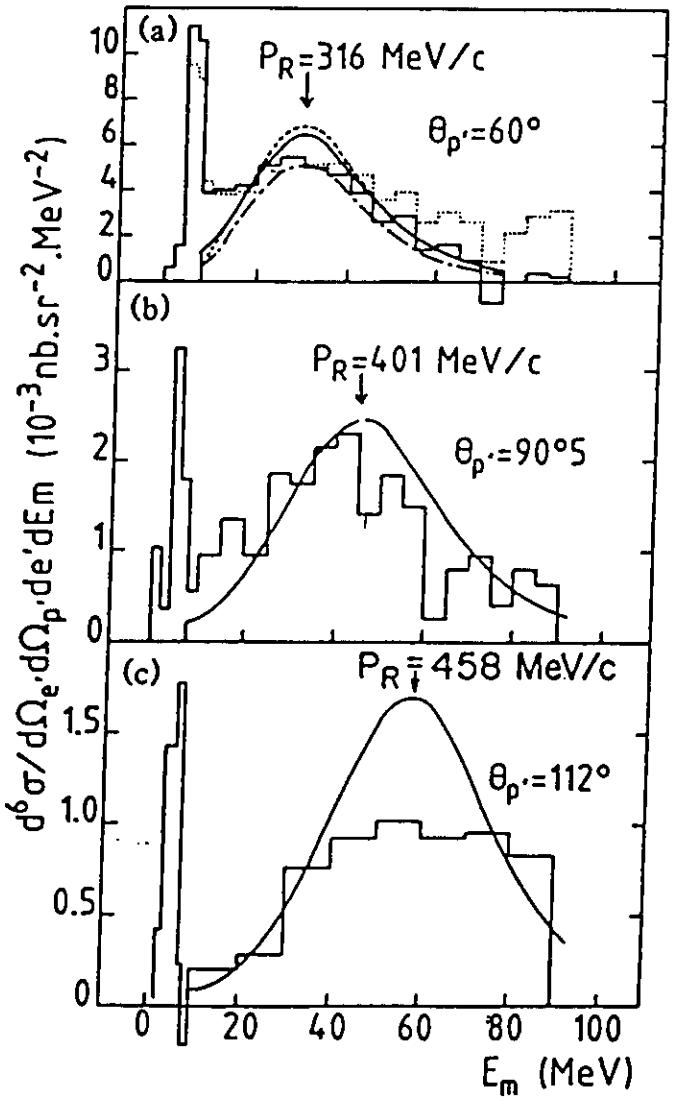
(a)
P_R=316 MeV/c
$\theta_{p'}$=60°
(b)
P_R=401 MeV/c
$\theta_{p'}$=90°5
(c)
P_R=458 MeV/c
$\theta_{p'}$=112°
$d^6\sigma/d\Omega_e \cdot d\Omega_{p'} \cdot de' dE_m$ (10^{-3}nb.sr^{-2}.MeV^{-2})
E_m (MeV)

Figure 4.

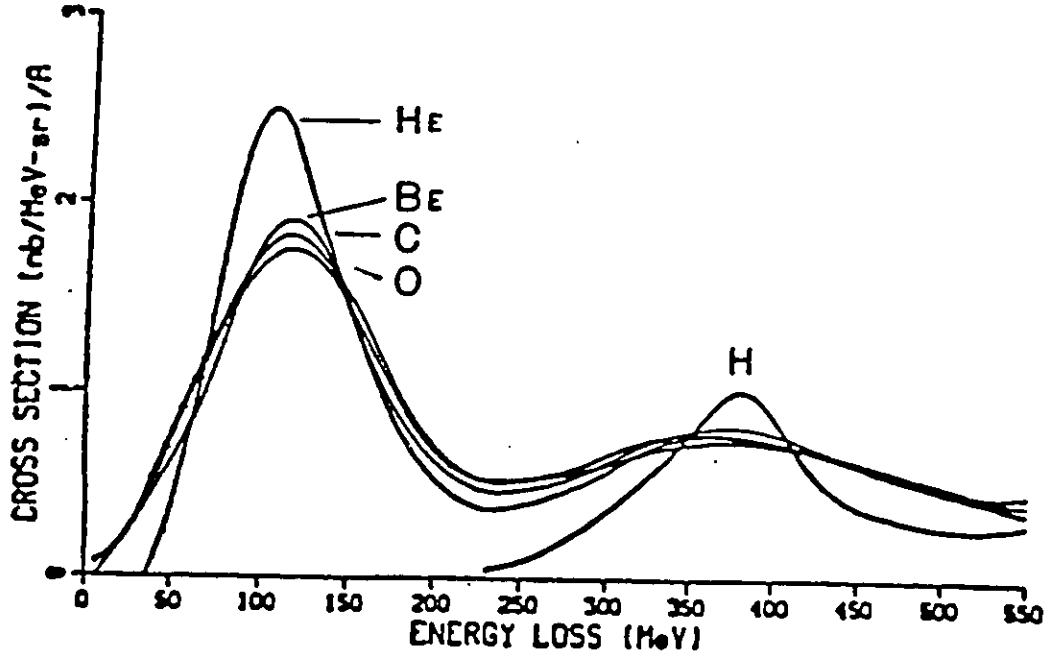
CROSS SECTION (mb/MeV-sr)/A
ENERGY LOSS (MeV)
HE
BE
C
O
H
0
50
100
150
200
250
300
350
400
450
500
550
1
2

Figure 5.

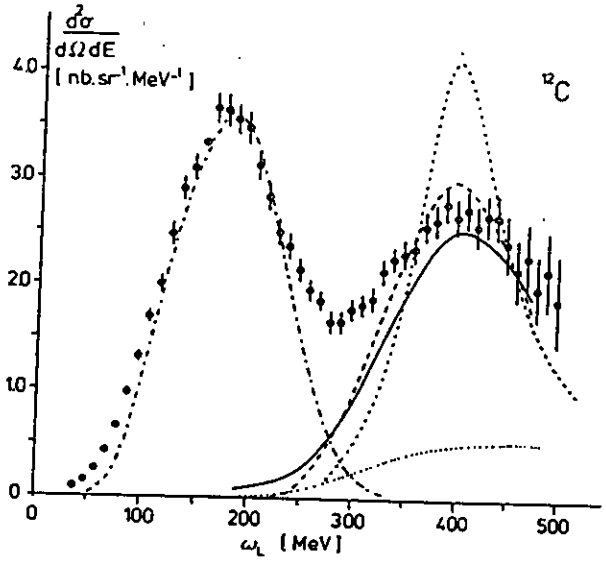

Figure 6.

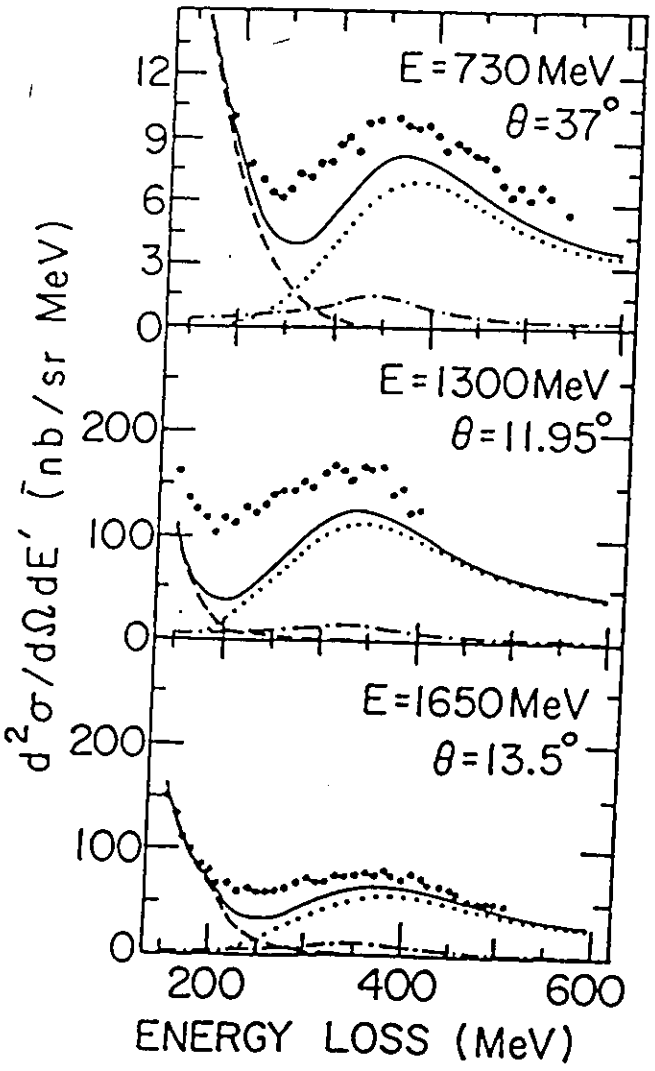

Figure 7.

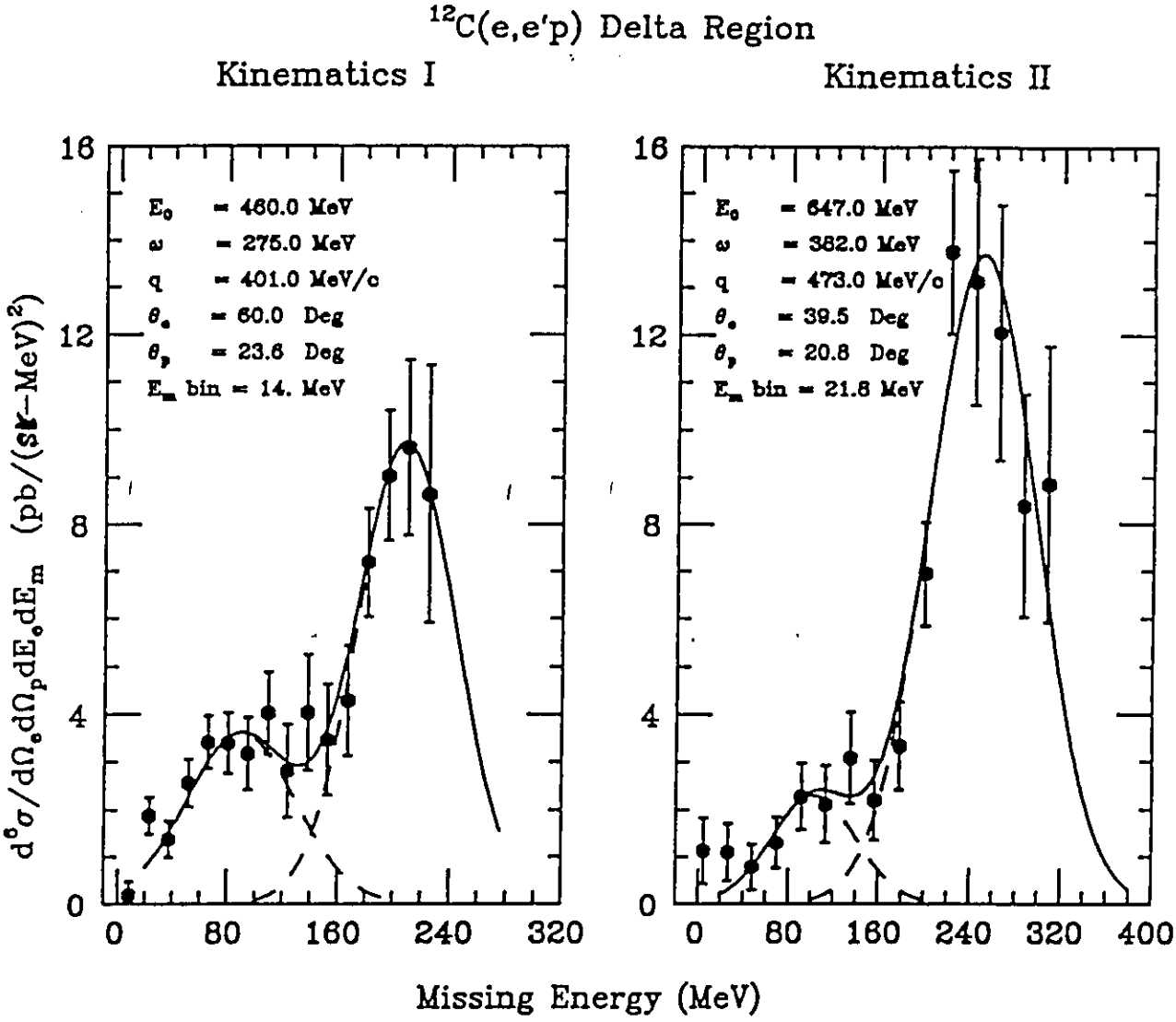
^{12}C(e,e'p) Delta Region
Kinematics I
Kinematics II
E_0 = 460.0 MeV
ω = 275.0 MeV
q = 401.0 MeV/c
θ_e = 60.0 Deg
θ_p = 23.6 Deg
E_m bin = 14. MeV
E_0 = 647.0 MeV
ω = 382.0 MeV
q = 473.0 MeV/c
θ_e = 39.5 Deg
θ_p = 20.8 Deg
E_m bin = 21.8 MeV
$d^6\sigma/d\Omega_e d\Omega_p dE_e dE_m$ (pb/(sr-MeV)^2)
Missing Energy (MeV)

Figure 8.

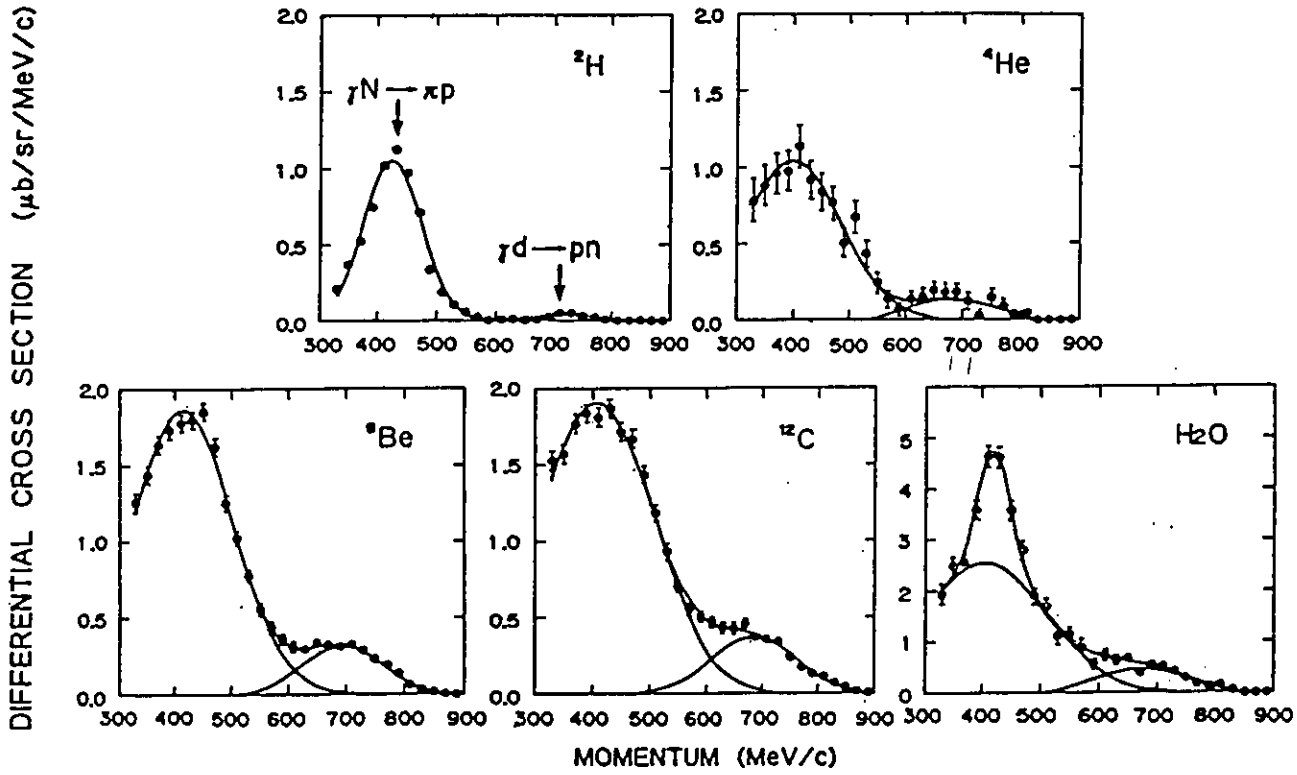
DIFFERENTIAL CROSS SECTION (μb/sr/MeV/c)
MOMENTUM (MeV/c)
²H
γN → πp
γd → pn
⁴He
⁹Be
¹²C
H₂O

Figure 9.

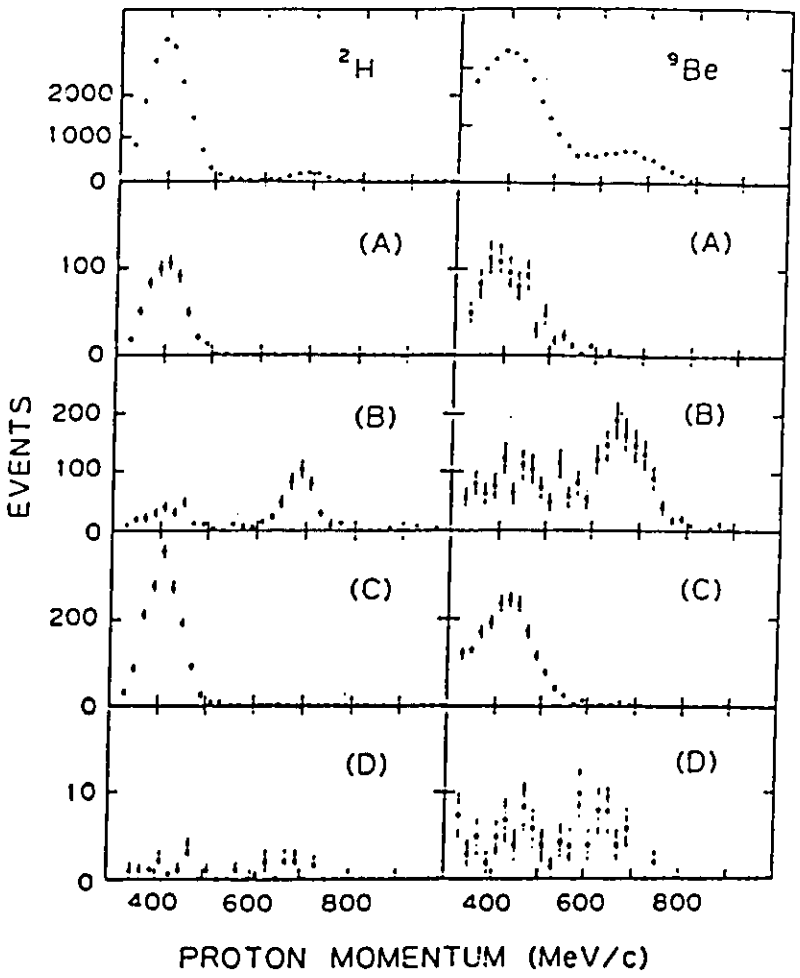
^{2}H
^{9}Be
2000
1000
0
(A)
(A)
100
0
(B)
(B)
200
100
0
(C)
(C)
200
0
(D)
(D)
10
0
EVENTS
400
600
800
400
600
800
PROTON MOMENTUM (MeV/c)

Figure 10.

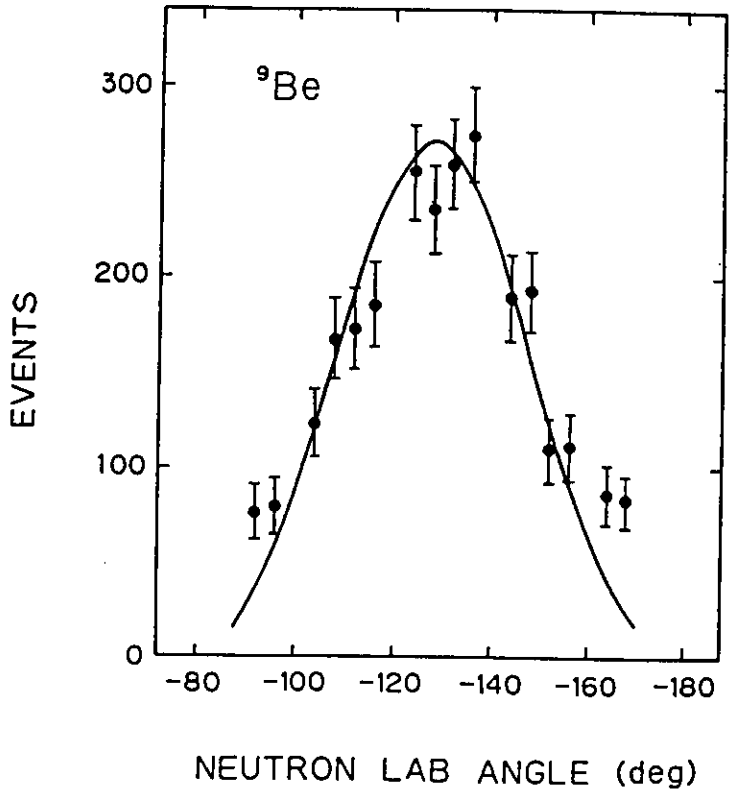

Figure 11.

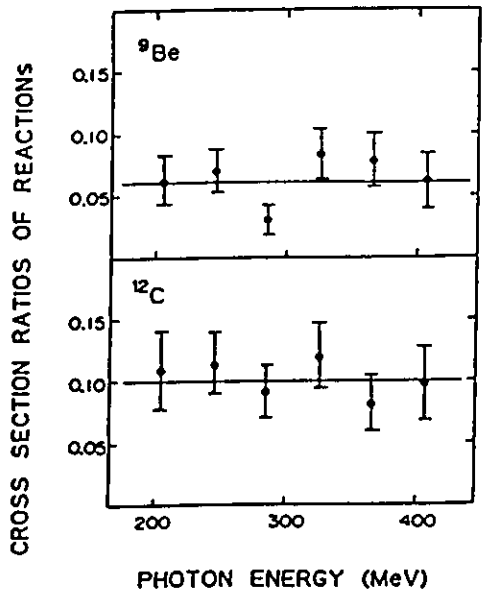

Figure 12.

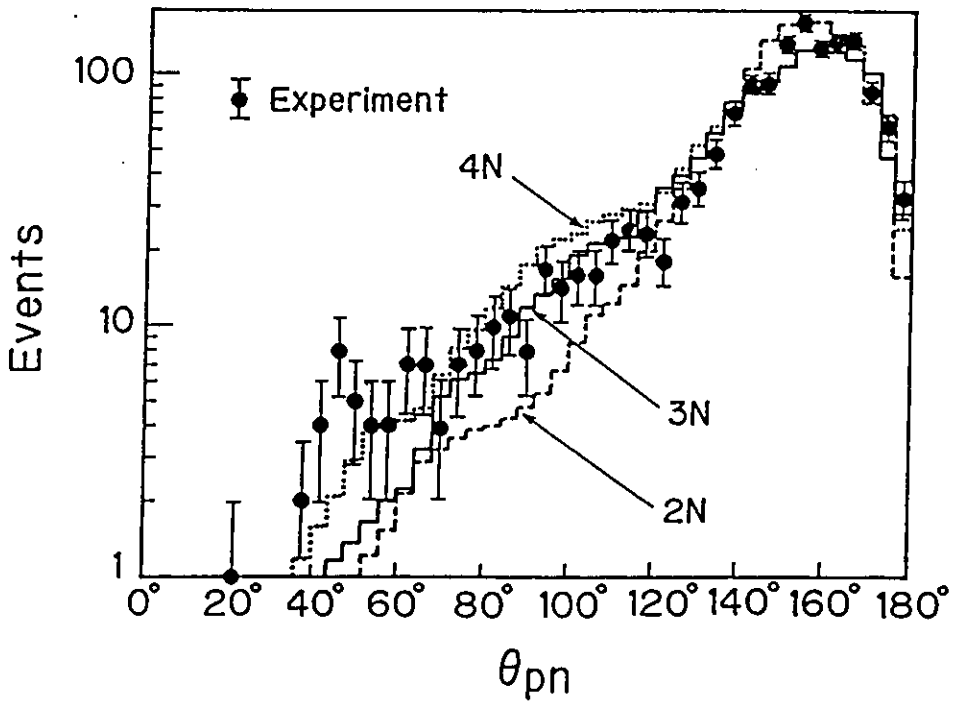

Figure 13.

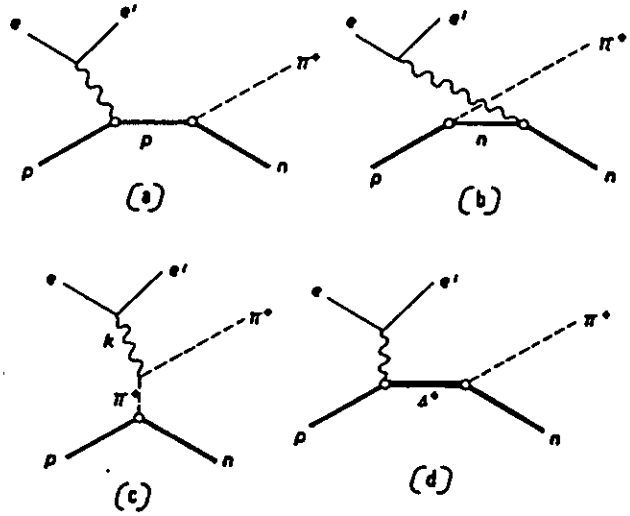

Figure 14.

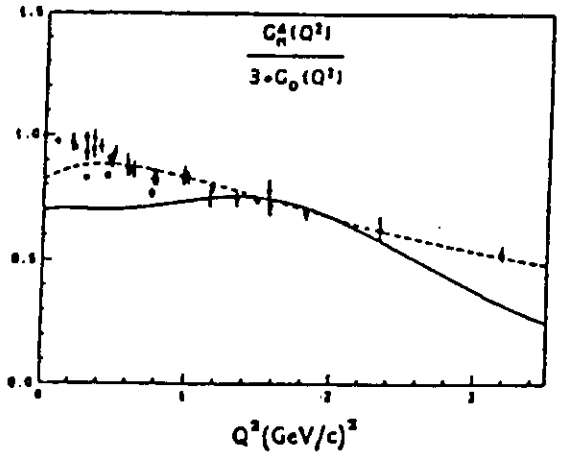

Figure 15.

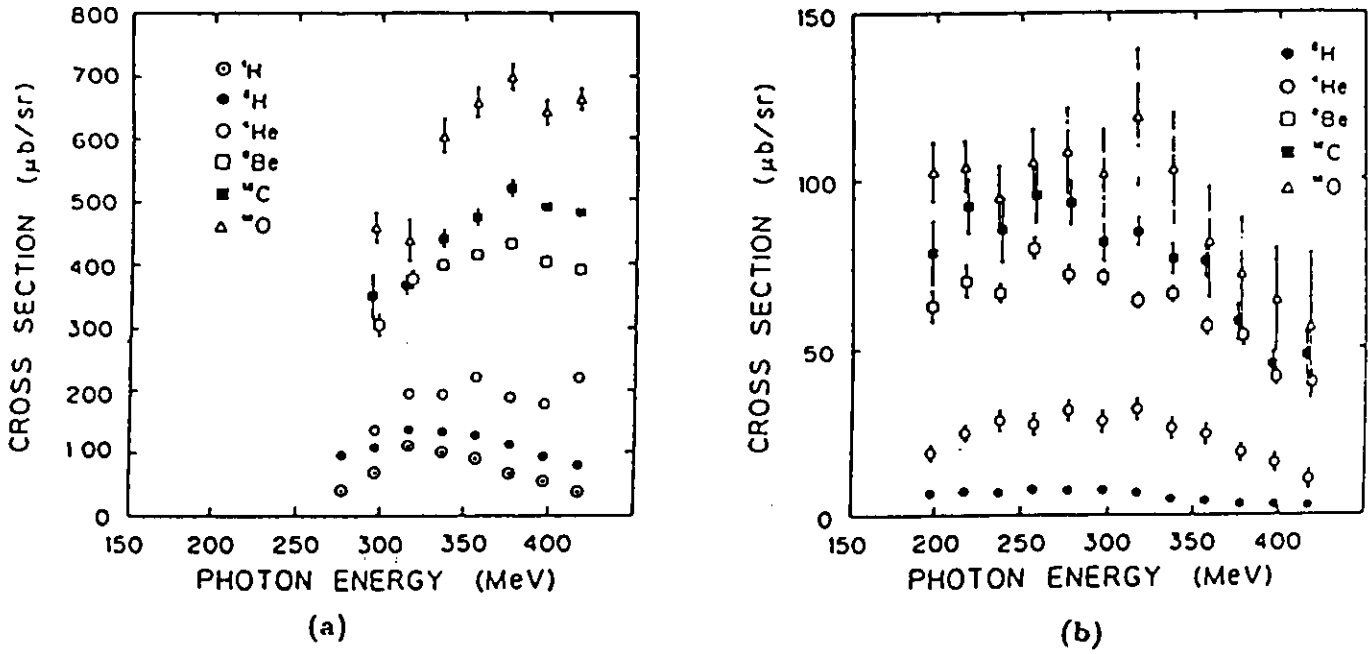

Figure 16.

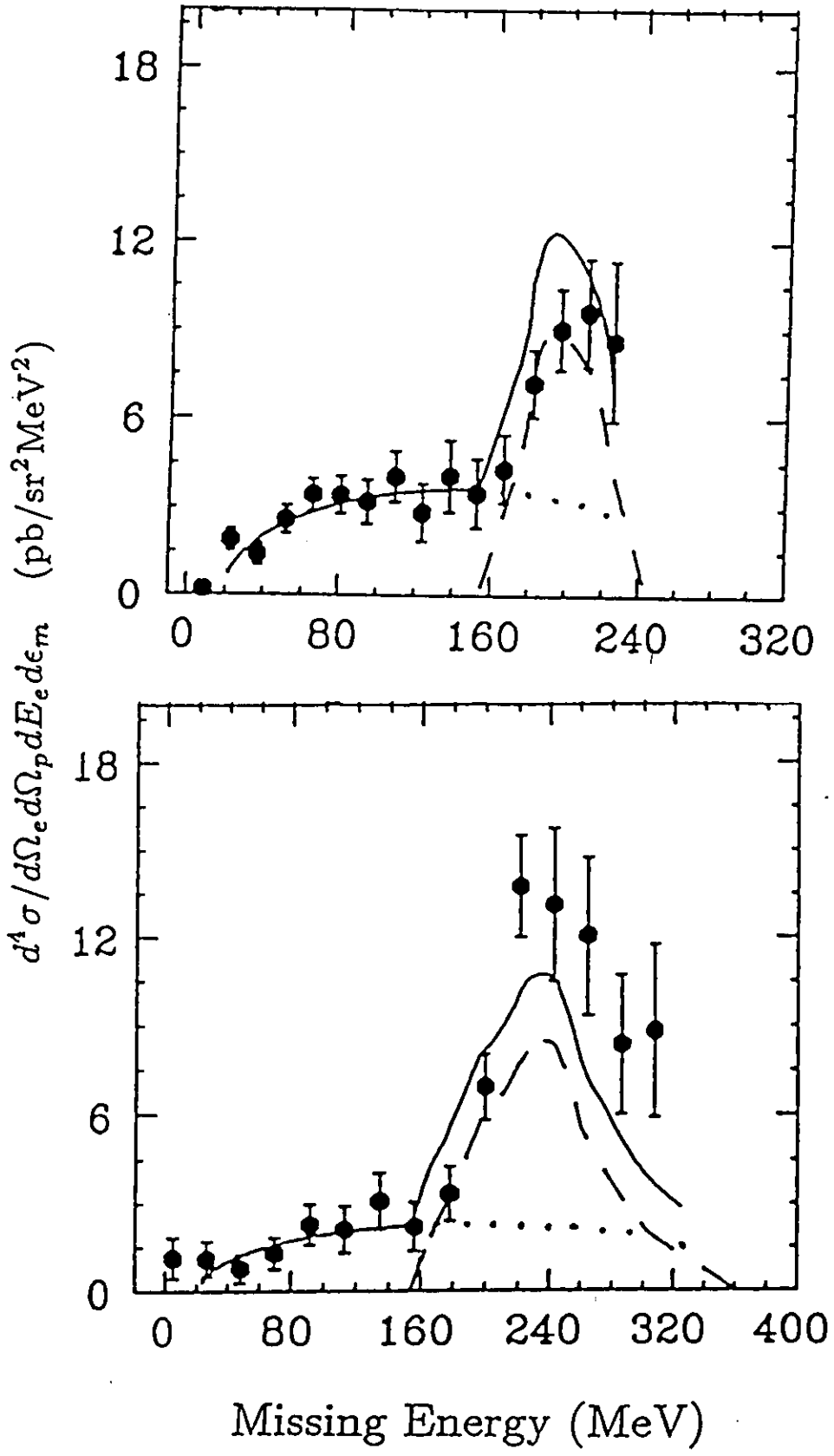
18
12
6
0
0
80
160
240
320
18
12
6
0
0
80
160
240
320
400
$d^4\sigma/d\Omega_e d\Omega_p dE_e d\epsilon_m$ (pb/sr^{2}MeV^2)
Missing Energy (MeV)

Figure 17.

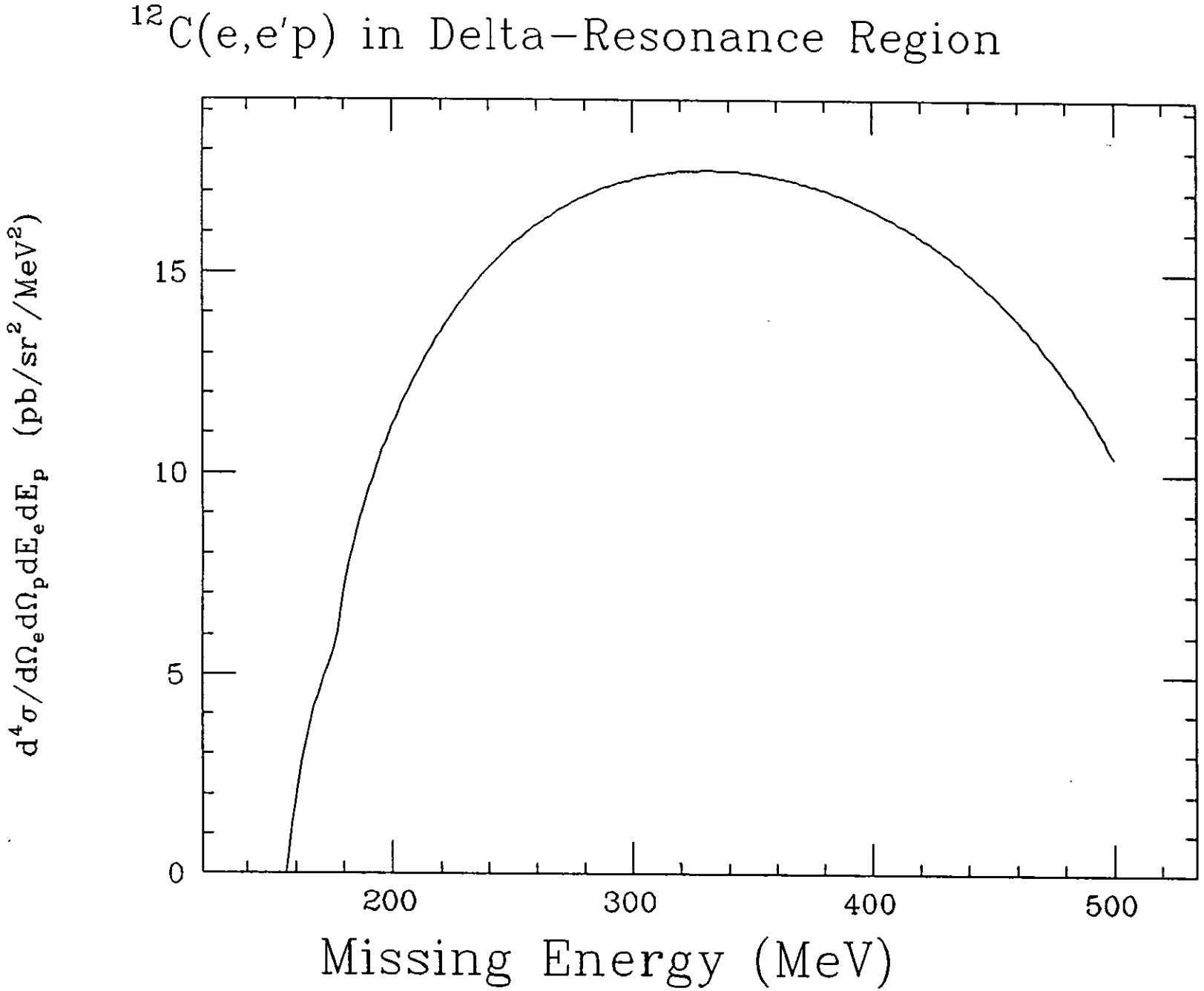
^{12}C(e,e'p) in Delta−Resonance Region
$d^4\sigma/d\Omega_e d\Omega_p dE_e dE_p$ (pb/sr^2/MeV^2)
0
5
10
15
200
300
400
500
Missing Energy (MeV)

Figure 18.

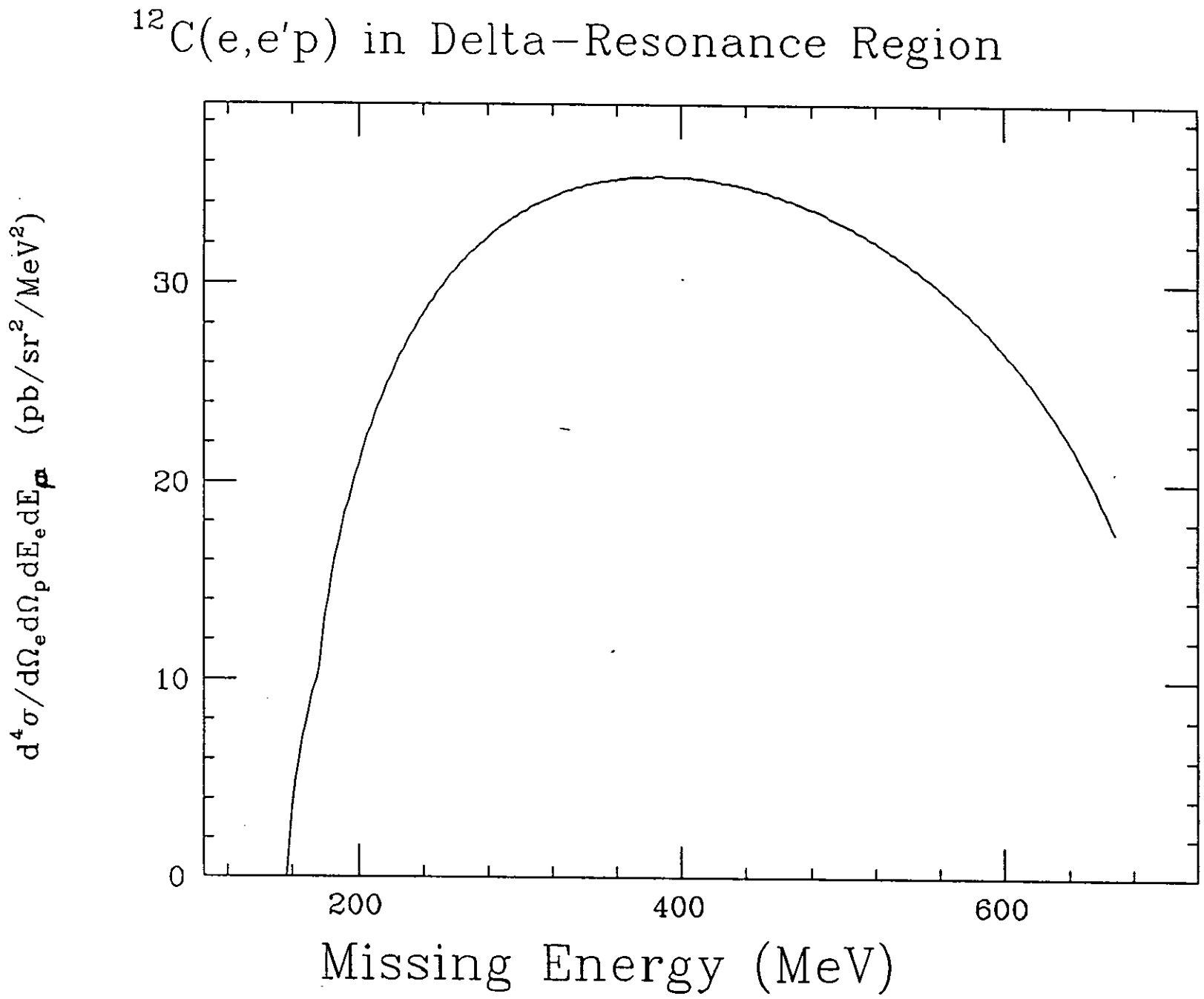
^{12}C(e,e'p) in Delta−Resonance Region
$d^4\sigma/d\Omega_e d\Omega_p dE_e dE_p$ (pb/sr^2/MeV^2)
0
10
20
30
200
400
600
Missing Energy (MeV)

Figure 19.